Wavefront correction of Ti : sapphire terawatt laser with varying precision of phase conjugation between deformable mirror and wavefront sensor*

Yu Liang-Hong(於亮红)[a], Liang Xiao-Yan(梁晓燕)[a]†, Ren Zhi-Jun(任志君)[a], Wang Li(王 利)[b], Xu Yi(许 毅)[a], Lu Xiao-Ming(陆效明)[a], and Yu Guo-Hao(于国浩)[b]

[a] *State Key Laboratory of High Field Laser Physics, Shanghai Institute of Optics and Fine Mechanics, Chinese Academy of Sciences, Shanghai* 201800, *China*

[b] *Joint Laboratory of High Power Laser Physics, Shanghai Institute of Optics and Fine Mechanics, Chinese Academy of Sciences, Shanghai* 201800, *China*

(Received 18 January 2011; revised manuscript received 6 June 2011)

The phase conjugation between the deformable mirror and the wavefront sensor in the aberration correction of a terawatt Ti:sapphire laser is studied experimentally and theoretically in this paper. At varying values of phase-conjugation precision, we focus the corresponding beams into spots of the same size of 5.1 μm × 5.3 μm with a $f/4$ parabola in the 32 TW/36 fs Ti:sapphire laser system. The results show that the precision of conjugation can induce an intensity modulation but does not significantly affect the wavefront correction.

Keywords: adaptive optics, wave front correction, phase conjugation, deformable mirror

PACS: 42.15.Dp, 42.60.–v, 42.60.Jf **DOI:** 10.1088/1674-1056/21/1/014201

1. Introduction

The chirped-pulse-amplification (CPA) technology has led to the improvement of tabletop lasers from terawatt (TW) to petawatt level with a pulse duration of a few tens of fs and even sub-10 fs.[1–3] These types of lasers are widely used to investigate high field laser–matter interactions, such as the generation of ultrafast X-ray radiation,[4,5] the high-order harmonic generation,[6–8] the laser wake field particle acceleration,[9] the laser-induced nuclear photophysics, and the fast ignition of laser fusion.[10,11] For most applications in ultrahigh field laser–matter interaction research, the intensity at focus is a key factor in addition to the peak power. Recent advances in fs laser sources are able to generate intensities approaching $\sim 10^{22}$ W/cm^2,[12,13] so the quality of the beam corresponding to a diffraction-limited spot size becomes crucial. With the terawatt laser, the intensity can also be improved to 10^{18}–10^{21} W/cm^2 by using a different focal mirror based on the wavefront active correction technology.[14,15]

The active correction of wavefront is a powerful method to reshape an irregular wavefront into a flat one, yielding a smaller focal spot after being focused by a lens. Recent studies have reported that a diffraction limitation (DL) focal spot with a full-width at half-maximum (FWHM) of 0.8 μm can be obtained with an $f/0.6$ off-axis parabola (OAP) and the adaptive optics wavefront correction on a 45-TW laser system.[16]

The adaptive optics system[17] (AOS) has two components: a correction device (usually a deformable mirror (DM))[18] and a wavefront sensor (a four-wave lateral shearing interferometer (SID4, PHASICS, France)). Normally, the conjugation between the deformable mirror and the sensor is crucial and should receive great attention. However, for most large laser systems, this is difficult to ensure because of the space limitations and the optic device sizes. In the present study, we investigate the requirements for the conjugation precision theoretically and experimentally based on our TW-fs laser system. The rest of this paper is organized as follows. In Section 2, we introduce the experimental setup, which is very different from the active wavefront correction system that is conventionally used. Theoretical simulations of the wavefront

*Project supported by the National Basic Research Program of China (Grant No. 2011CB808101) and the National Natural Science Foundation of China (Grant No. 60921004).

†Corresponding author. E-mail: liangxy@mail.siom.ac.cn

© 2012 Chinese Physical Society and IOP Publishing Ltd

distribution and the intensity modulation away from the conjugated plane are presented in Section 3. Section 4 is devoted to the experimental studies of the wavefront corrections for two cases: one with strict phase conjugation and the other with phase conjugations at different precisions. Finally, the conclusions drawn from the present study are given in Section 5.

2. Experimental scheme

The TW laser system is characterized by a typical CPA configuration based on a Ti:sapphire crystal, which can deliver a pulse with a peak power of 32 TW and duration of 36 fs at the 10 Hz operation.[19] It consists of an oscillator, a pulse stretcher, a regenerative amplifier, two stages of multi-pass amplifiers, and a pulse compressor in a vacuum chamber. The focus optics is an $f/4$ OAP with a clear aperture (50 mm) matching the beam size.

The experimental setup of the active wavefront correction system is shown in Fig. 1. In the experiment, we explore a new scheme, where the AO loop is constructed by placing a SID4 directly behind the focus of the OAP on the direct beam line. Therefore, no additional aberration from the collimated optics and the alignment is introduced, and the measured values can reveal the phase near the focus more accurately. To measure the wavefront and the focal spot simultaneously, we use a beam splitter to divide the beam into two parts. One part is sent to the SID4 for the wavefront measurement, and the other is sent to a charge couple device (CCD) for the focus size measurement. Since the SID4 is placed directly behind the focus of the OAP the defocus results in a divergent wavefront that cannot be directly compared with a flat one. To obtain the real wavefront, the defocus is subtracted, and the wavefront is compared with a flat one to generate an error signal. The AO loop software is used to convert the wavefront error signal into voltages that control the shape of the deformable mirror. After being corrected by the deformable mirror, the wavefront turns approximately flat, and a nearly diffraction-limited focal spot will be obtained after being focused by the OAP.

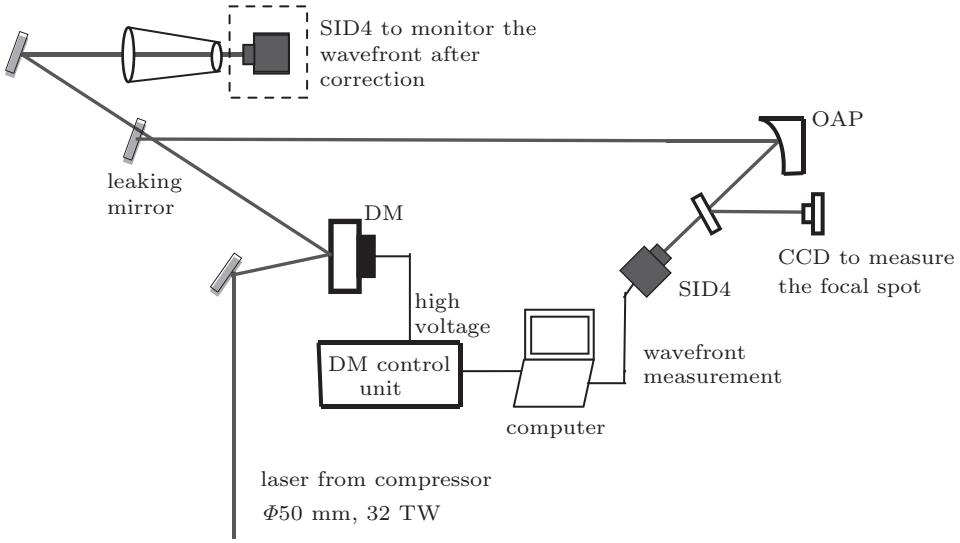


Fig. 1. Exprimental setup of wavefront correction on the Ti:sapphire CPA laser.

3. Theoretical simulation of wavefront distribution and intensity modulation at conjugated plane

Figure 2 can be used to analyse the cases of different values of phase-conjugation precision. We use an equivalent lens with a clear aperture (D) of 50 mm and a focal length (f) of 200 mm to represent the OAP. For effective comparison, the diameter of the SID4 entrance pupil is kept at a constant, and the distance between the lens and the sensor is fixed in the practical application.

When the DM and the wavefront sensor are phase-conjugated, they can be described by the fol-

lowing formulas of geometrical optics:

$$\frac{1}{u}+\frac{1}{v}=\frac{1}{f}, \tag{1}$$

$$\frac{v}{u}=\frac{d}{D}, \tag{2}$$

where u is the objective distance, v is the image distance, and $d = 3.5$ mm is the diameter of the SID4 entrance pupil. When $f = 200$ mm and $D = 50$ mm, the solutions of the above equations are $u_0 = 3057$ mm and $v_0 = 214$ mm, corresponding to the phase-conjugated planes.

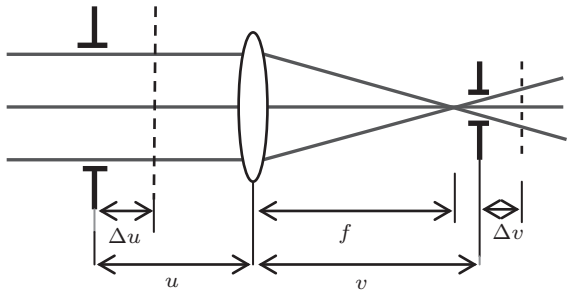


Fig. 2. Schematic diagram used for analyzing different values of phase-conjugation precision, parameters are specified in the main text.

When the SID4 is moved by Δv from v_0, equation (2) can be expressed as

$$\frac{v}{u}=\beta=\frac{v_0+\Delta v-f}{f}, \tag{3}$$

where β is the amplification factor, Δu is the distance between the DM and the plane of u_0, and Δv is the distance between the sensor and the plane of v_0. For Δu and Δv, positive values represent moving away from the lens, and negative values represent moving towards the lens. To maintain the phase-conjugation, the objective distance is

$$u=f+\frac{f^2}{v_0+\Delta v-f}. \tag{4}$$

For instance, when the SID4 is moved by 1 mm toward the right and away from v_0 ($\Delta v = 1$ mm), then Δu must be -190 mm to obtain the phase conjugation. Likewise, if $\Delta v = -1$ mm, Δu should be 220 mm. In other words, when the SID4 is moved toward the right (left) by 1 mm, the DM should be moved toward the right (left) by 190 mm (220 mm) to guarantee the phase conjugation. Similarly, when the DM is moved toward the right (left) by 190 mm (220 mm), the SID4 should be moved toward the right (left) only by 1 mm. We find that a very fine displacement of the sensor corresponds to a nearly 200-fold displacement of the DM.

Then, we study the evolutions of the wavefront and the intensity after passing through the phase-conjugation plane. We use an advanced physical optics analysis code GLAD to model this process. The code is designed to analyse beam trains and laser devices, including the effects of diffraction, active medium, lens and mirror, and aberration. The initial wavefront and the initial intensity distribution are measured with the sensor fixed at $v_0 = 214$ mm when the phase conjugation between the DM and the sensor is maintained. The model reveals the evolutions of the wavefront and the intensity profiles after 1 mm, 2 mm, and 4 mm of free propagation from the plane of v_0 (Fig. 3). The peak-to-valley (PTV) value of the initial wavefront is 1.485λ. It turns to 1.492λ after 1 mm, 1.490λ after 2 mm, and 1.502λ after 4 mm of free propagation. The PTV values and the wavefront shapes (Fig. 3) demonstrate that the wavefront distributions at different values of phase-conjugation precision remain almost the same. However, the variations in the intensity modulation are very significant. The simulation results show that the intensity modulation depth is about 15% at the initial position (Fig. 3(a)) and reaches 35% after 4 mm of free space propagation (Fig. 3(d)). The intensity modulation is enhanced with the increase of distance of free propagation from the conjugated plane, whereas the wavefront distribution is almost unchanged, remaining in the range of effective correction. The intensity modulation is very harmful to sensitive optic elements, the precision of phase conjugation should be controlled to regulate the depth of the intensity modulation within a safe range. In addition, we are also concerned about the wavefront correction results at different values of precision of phase-conjugation. These are experimentally studied in the next section.

Equation (4) shows that when the sensor is moved toward the right by 1 mm, the DM should be moved by 190 mm to guarantee the phase conjugation. This indicates that when the sensor is fixed at v_0, the location of the DM may be in a very wide range, and the effectiveness of correction is not disturbed. Therefore, the position of the DM is not critical for our experimental scheme, which is very convenient for practical applications.

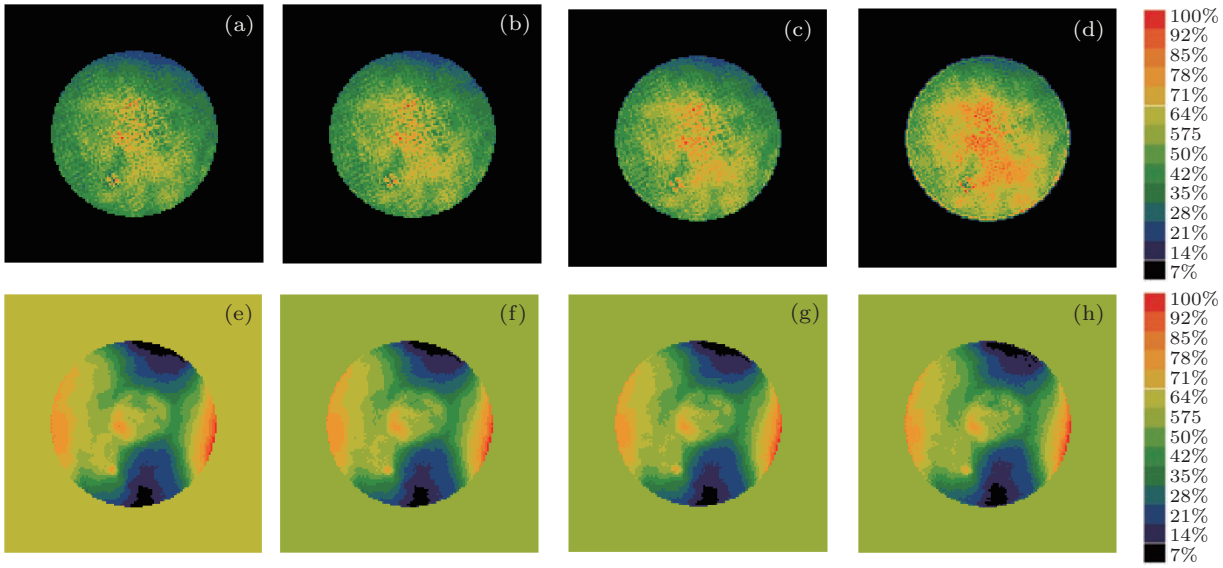


Fig. 3. (colour online) Intensity and wavefront profiles modeled by the GLAD when beam is allowed 0 mm ((a) and (e)), 1 mm ((b) and (f)), 2 mm ((c) and (g)), and 4 mm ((d) and (h)) of free space propagation from the conjugated plane. The upper panels show the intensity distributions, while the lower panels show the wavefront profiles.

4. Experimental study of wavefront correction

4.1. Wavefront correction when phase between DM and sensor is conjugated

The wavefront and the focal spot when the DM is conjugated with the sensor are measured. Figure 4(a) is a three-dimensional (3D) view of the wavefront before the correction, which has a PTV value of 1.485λ and an RMS value of 0.186λ. The aberrations without correction are mainly from the astigmatism at 45° with a coefficient value of -0.145λ and the coma at the x axis with a coefficient of 0.069λ, thus inducing a high PTV value. The Strehl ratio of the focal spot is 0.3. The focal spot after a 200-mm focal length OAP mirror is recorded with a CCD camera. Figure 4(b) shows the focal spot before the correction, which has a size of 8.9 μm × 9.6 μm at FWHM and is 2.3-fold of the diffraction limitation. Figure 4(c) illustrates the focal spot lineouts along the x and the y axes.

After the correction, the coefficient of the astigmatism at 45° decreases to -0.012λ, and the coma at the x axis decreases to 0.001λ. The 3D view of the wavefront after the correction, with a PTV value of 0.472λ and an RMS value of 0.047λ, is shown in Fig. 5(a). The focal spot after a 200-mm focal length OAP with a focal spot size of 5.1 μm × 5.3 μm is 1.36-fold of the diffraction limitation (Fig. 5(b)). The results indicate that the wavefront correction improves the peak intensity in the focal plane by a factor greater than 2.5. The shape of the focus becomes more symmetrical, which is very important for some physics experiments. Figure 5(c) shows the focal spot lineouts along the x and the y axes.

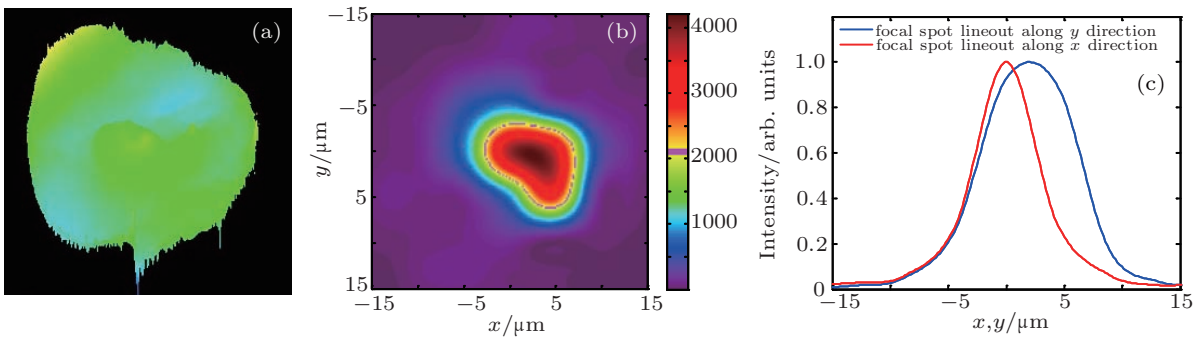


Fig. 4. (colour online) (a) The 3D view of wavefront before the correction. The PTV value is up to 1.485λ, and the RMS is 0.186λ. (b) Laser focal spot after a 200-mm focal length OAP. Spot size is 8.9 μm × 9.6 μm at FWHM, and the Strehl ratio is 0.3. (c) Focal spot lineouts along the x and the y axes.

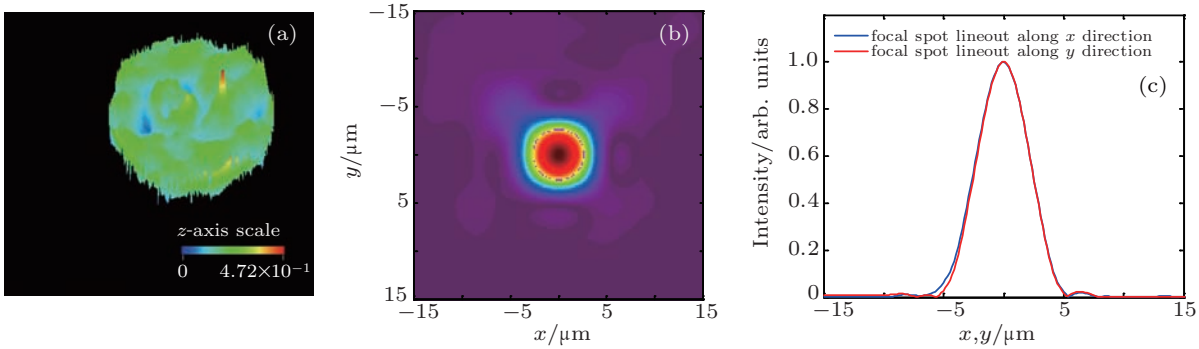


Fig. 5. (colour online) (a) The 3D view of wavefront after the correction. The PTV value is 0.472λ, and the RMS is 0.047λ. (b) Laser focal spot after a 200-mm focal length OAP with a spot size of 5.1 μm × 5.3 μm at FWHM. The Strehl ratio is 0.91. (c) Focal spot lineouts along the x and the y axes.

4.2. Wavefront correction when phase conjugation between DM and sensor is at different precisions

In Section 3, we conclude that the wavefront is almost unchanged while the intensity is modulated when the beam is away from the conjugation plane. We perform the following experiments to identify the effect on the wavefront correction when the precise phase conjugation is not maintained. Although the intensity modulation is very harmful to some sensitive optical elements, the depth of modulation can be maintained below the damage threshold of the sensor. In this study, we correct the wavefront and activate the active loop when the sensor is fixed while the DM deviates from the conjugated plane.

To match the beam size with the sensor pupil, the sensor is fixed at $v_0 = 214$ mm. The DM is located respectively at three different positions, i.e., 2867 mm, 2700 mm, and 2420 mm, which are away from the conjugated plane of the sensor by distances of 190 mm, 357 mm, and 637 mm, respectively. From Eqs. (1) and (3), we find that the three positions selected correspond to the conjugated planes of $v = 215$ mm, $v = 216$ mm, and $v = 218$ mm, respectively. Results of the correction are shown in Fig. 6. Corrected wavefronts have almost similar RMS values ranging from 0.047λ to 0.050λ, whereas the focal spot size is maintained at ∼ 5.3 μm × 5.3 μm. Table 1 presents the measured results after the correction. The distributions of the wavefront and the focal spots are not disturbed when the phase-conjugation between the DM and the sensor have different values of precision.

Figure 6 demonstrates that the focal spot sizes and the wavefronts after the correction are almost the same even the DM is placed at different positions, indicating insignificant differences in the range of the pulse fluctuation. However, the measured intensities show a notable modulation with the deviation of the phase conjugation. We use the sensor to measure the normalized intensity profiles along the x axis when the DM is placed at different locations (Fig. 7). The initial normalized intensity profile with the phase conjugation has a modulation depth of about 18%, and it increases to 25% and 35% when the DM deviates from the conjugated plane by 190 mm and 357 mm, respectively. The largest modulation (about 50%) is obtained when the DM deviates from the conjugated plane by 637 mm. The findings suggest that the intensity modulation increases as the DM deviation from the conjugated plane increases. The escalation of the intensity modulation will increase the risk of damage to the sensor.

Table 1. Results of active correction when the DM is at different positions.

DM position/mm	PTV/λ	RMS/λ	Size of focal spot/μm^2	Depth of intensity modulation
No correction	1.485	0.186	8.9×9.6	
3057	0.472	0.047	5.1×5.3	18%
2867	0.498	0.048	5.2×5.4	25%
2700	0.485	0.050	5.3×5.4	35%
2420	0.522	0.047	5.3×5.3	50%

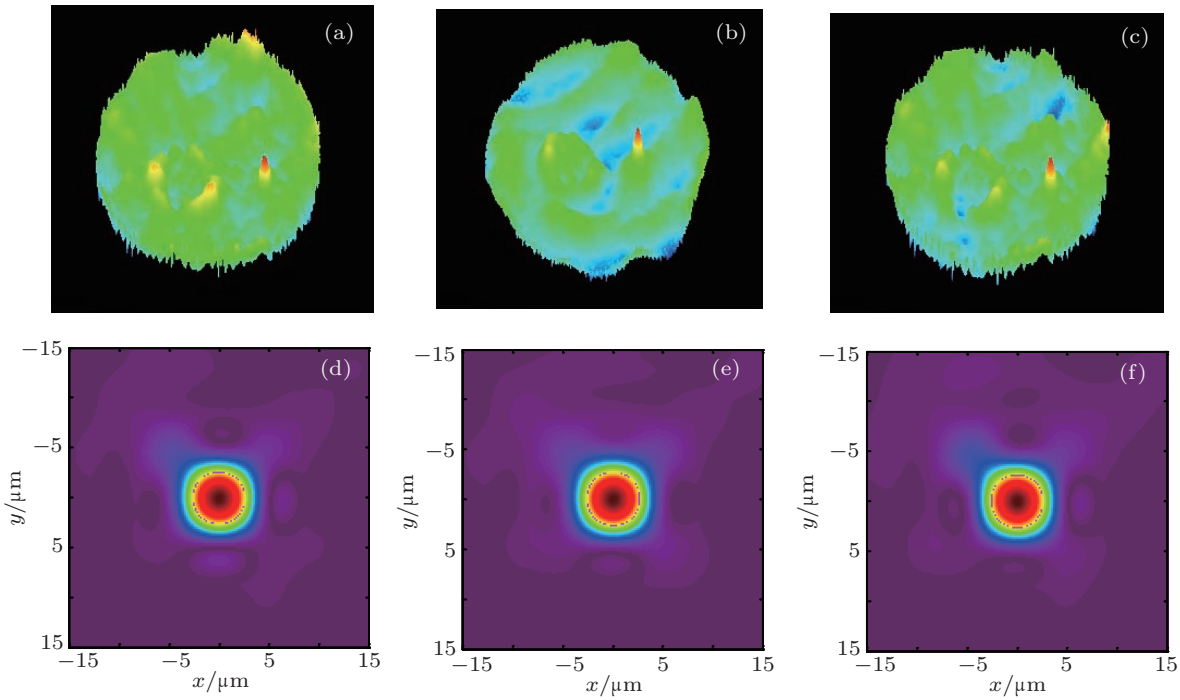


Fig. 6. (colour online) Wavefronts (upper) and corrected focal spot distributions (bottom) measured when the DM is placed at the planes of ((a) and (d)) $u = 2867$ mm, ((b) and (e)) $u = 2700$ mm, and ((c) and (f)) $u = 2420$ mm.

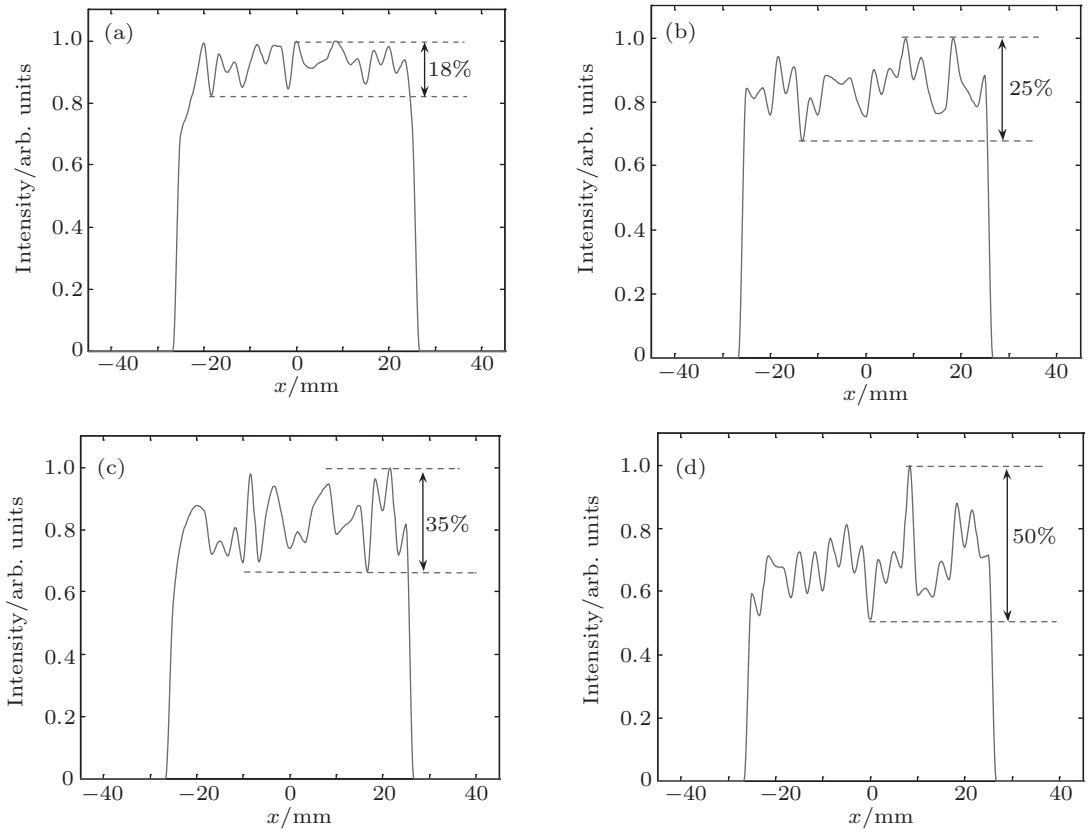


Fig. 7. Normalized intensity profiles along the x axis when DM deviates (a) 0 mm, (b) 190 mm, (c) 357 mm, and (d) 637 mm away from the conjugated plane. Intensity modulation has a depth ranging from 18% to 50%.

The results shown in Table 1 reveal that the corrected wavefronts and the focal spots with the precision of the phase conjugation at different values are almost the same as those with the strict phase conjugation. Our results indicate that the requirement for precision of conjugation in the wavefront correction is not very strict. The findings suggest that in order to prevent damage to the optic element by regulating the intensity modulation, we have a large range of locations for the DM without disturbing the effectiveness of correction. This is very convenient for practical applications.

5. Conclusion

In this study, we investigate the phase conjugation between the deformable mirror and the sensor in the wavefront correction of a TW laser system. The results show that the wavefront distribution is almost unchanged while the intensity is modulated when the phase conjugation has different precision values. The wavefront correction is not affected by a slight unconjugation between the DM and the wavefront sensor. When the DM deviation is within 637 mm, no evident change in the focal spots can be detected, and the size (5.3 μm × 5.3 μm) is 1.36-fold of the diffraction limitation after the correction. However, the intensity modulation is very sensitive to the change in the DM position, so the precision of the phase conjugation should be controlled to maintain the intensity modulation below the damage threshold of the sensor. The findings of this study are conducible to the construction of a convenient and effective adaptive loop for practical applications.

References

[1] Liang X Y, Leng Y X, Wang C, Li C, Lin L H, Zhao B Z, Jiang Y H, Lu X M, Hu M Y, Zhang C M, Lu H H, Yin D J, Jiang Y L, Lu X Q, Wei H, Zhu J Q, Li R X and Xu Z Z 2007 *Opt. Express* **15** 15335

[2] Chen X W, Leng Y X, Zhu Y, Li R X and Xu Z Z 2006 *Opt. Commun.* **259** 331

[3] Chen X W, Li X F, Liu J, Wei P F, Ge X C, Li R X and Xu Z Z 2007 *Opt. Lett.* **32** 2402

[4] Umstadter D, Chen S Y, Maksimchuk A, Mourou G and Wagner R 1996 *Science* **273** 472

[5] Workman J, Maksimchuk A, Liu X, Ellenberger U, Coe J S, Chien C Y and Umstadter D 1995 *Phys. Rev. Lett.* **75** 2324

[6] Zheng Y H, Zeng Z N, Xiong H, Li R X, Xu Z Z, Peng Y, Yang X and Zen H P 2009 *Appl. Phys. Lett.* **95** 141102

[7] Zheng Y H, Zeng Z N, Zou P, Zhang Li, Li X F, Liu P, Li R X and Xu Z Z 2009 *Phys. Rev. Lett.* **103** 043904

[8] Zheng Y H, Zeng Z N, Li X F, Chen X W, Liu P, Xiong H, Lu H, Zhao S T, Wei P F, Zhang L, Wang Z G, Liu J, Cheng Y, Li R X and Xu Z Z 2008 *Opt. Lett.* **33** 234

[9] Macklin J J, Kmetec J D and Gordon C L 1993 *Phys. Rev. Lett.* **70** 766

[10] Tabak M, Hammer J, Glinsky M E, Kruer W L, Wilks S C, Woodworth J, Campbell E M, Perry M D and Mason R J 1994 *Phys. Plasmas* **1** 1626

[11] Deutsch C, Furukawa H, Mima K, Murakami M and Nishihara K 1996 *Phys. Rev. Lett.* **77** 2483

[12] Hatchett S P, Brown C G, Cowan T E, Henry E A, Johnson J S, Key M H, Koch J A, Langdon A B, Lasinski B F, Lee R W, Machinnon A J, Pennington D M, Perry M D, Philips T W, Roth M, Sangster T C, Singh M S, Snavely R A, Stoyer M A, Wilks S C and Yasuike K 2000 *Phys. Plasmas* **7** 2076

[13] Wilks S C, Langdon A B, Cowan T E, Roth M, Singh M, Hatchett S, Key M H, Pennington D, MacKinnon A and Snavely R A 2001 *Phys. Plasmas* **8** 542

[14] Planchon T A, Rousseau J P, Burgy F, Che'riaux G and Chambaret J P 2005 *Opt. Commun.* **252** 222

[15] Fourmaux S, Payeur S, Alexandrov A, Serbanescu C, Martin F, Ozaki T, Kudryashov A and Kieffer J C 2008 *Opt. Express* **16** 11987

[16] Bahk S W, Rousseau P, Planchon T A, Chvykov V, Kalintchenko G, Maksimchuk A, Mourou G A and Yanovsky V 2004 *Opt. Lett.* **29** 2837

[17] Liu C, Mu Q Q, Hu L F, Cao Z L and Xuan L 2010 *Chin. Phys.* B **19** 064214

[18] Ning Y, Zhou H, Yu H, Rao C H and Jiang W H 2009 *Chin. Phys.* B **18** 1089

[19] Liang X Y, Leng Y X, Lin L H, Lu H H, Wang W T, Jiang Y H, Shuai B, Peng H L, Zhao B Z, Wang C, Zhang W Q, Zhang Z Q, Li R X and Xu Z Z 2006 *Opt. Lasers Eng.* **44** 130